Chapter 38
GHRS Data Analysis

In This Chapter...

38.1 The Post-COSTAR Point Spread Function

The post-COSTAR point spread function (PSF) has a sharp core and weak wings. Observations through the SSA show a Gaussian core with a FWHM of 0.975 diodes and wings that fall off (in intensity) as r^{-3} at radii larger than 1 arcsec. When this measured profile is deconvolved from the square SSA aperture, we find a sharp core with a FWHM of about 0.375 diodes—this amounts to about 0.08 arcsec. For a detailed description of the analysis of the PSF please see, Robinson, R. "Investigating the Post-COSTAR Point Spread Function for the GHRS" in *Calibrating Hubble Space Telescope: Post Servicing Mission*, 1995.

During preflight testing of COSTAR, the GHRS mirrors were contaminated by fine dust particles. Light scattering was expected to be a problem at the radial distance of 2 to 3 arcsec. The first Servicing Mission Orbital Verification (SMOV) observations agreed moderately with the light scattering theoretical expectations. Special observations were obtained in Cycle 4 and 5 to measure this scattered light.

The observing plan for the special observations was to center up on the target star, back off 0.2 arcsec, and scan across the star out to a radial distance of 3.0 arcseconds. The first dwell position at radial distance of –0.2 arcsec from the SSA acquisition position was chosen so the scan would sample both sides of the PSF. A scan with nine dwell positions was defined. The target was centered in the SSA with an ACQ/PEAKUP before the start of each SCAN. Three SCANs were obtained, two were in the $-x$ direction at a wavelengths of 1400 Å and 2700 Å and one was in the $+y$ direction at 2700 Å. A previous scan in y at 1400 Å already existed.

The light entering the FOC (OTA+COSTAR) is a close match to the light entering the GHRS. Model FOC PSF images were created using TinyTim. Models were created to match the GHRS 1400 Å (FOC F140M filter) and the 2700 Å (FOC F278M filter) observations, see Figure 38.1 in which model profiles are offset by one pixel. The FOC model PSF pixel scale is 0.0143 arcsec/pixel (*f*/96). A square aperture (15 pixels on a side) was walked across the model PSF images to match the scan positions of the GHRS observations. A plot of the sum of the counts in this aperture at each position should represent the measured PSF envelope extracted from the GHRS observations. The model points were scaled to match the GHRS second dwell position points.

A good match was found between the FOC model scan points and the first four GHRS dwell positions in each scan. Beyond dwell position #4 (1.0 arcsec), the counts in the model scan continue to fall off in intensity while the counts in the GHRS scan level off. The GHRS profile beyond 1.0 arcsec suggests higher scattered light than is predicted by the FOC PSF model. It is unlikely that these profile wings are due to detector noise because the counts detected are significant and well above normal background levels.

The FOC model fit, of course, is not intended to represent the actual GHRS PSF, but instead to determine the position of the star relative to the GHRS scan. However, comparisons of the FOC model scans with the actual GHRS scans do show some similarities as well as some discrepancies that are worth noting.

First, the –*x*-axis scans indicate the GHRS PSF within the region <1.0 arcsec is slightly broader at 1400 Å than at 2700 Å. This broadening of the profile may be due to a halo effect at 1400 Å that is not present at 2700 Å. This broadening appears to be in both the actual GHRS scans and the FOC model scans which suggests it is possibly related to the COSTAR optics. The 1400 Å scan starts to diverge from the FOC model at ~1.0 arcsec, while the 2700 Å scan tracks the FOC model scan out to a distance of ~1.4 arcsec before diverging from the model scan. This would indicate the onset of scattering is more pronounced at 1400 Å than at 2700 Å.

Second, the +*y*-axis scan at 2700 Å shows a narrower inner core to the profile compared to the –*x*-axis scan profiles. This result is possibly due to the inferred large offset (~0.050 arcsec) introduced in the positioning of the +*y*-axis spatial scan. This only indicates the target star was more centered in the aperture at dwell position #2 for the +*y*-axis scan than for the –*x*-axis scans. If the +*y*-axis and –*x*-axis scans at 2700 Å are overlaid and moved vertically so as to match the counts at dwell position #4, the fall off in the profiles are nearly identical. This suggests the far wings of the PSF are symmetrical at 2700 Å. The –*x*-axis scan, which has better positioning to measure the wings of the PSF, is a good indicator of the fall off in the wings of the GHRS PSF.

The observations at both 1400 and 2700 Å demonstrate that the GHRS PSF has extended wings. These do not rise above the expected (FOC) level until one is at about 1% of the peak intensity for a star, therefore these wings are unlikely to contaminate the spectrum of a nearby star in a significant way except when there is a large (~5 magnitude) difference in brightness. The information provided in the figures and tables should allow a first-order correction to be made in such cases if spectra of both objects exist.

Figure 38.1: Observed GHRS Profiles vs. TinyTim Models From FOC Parameters

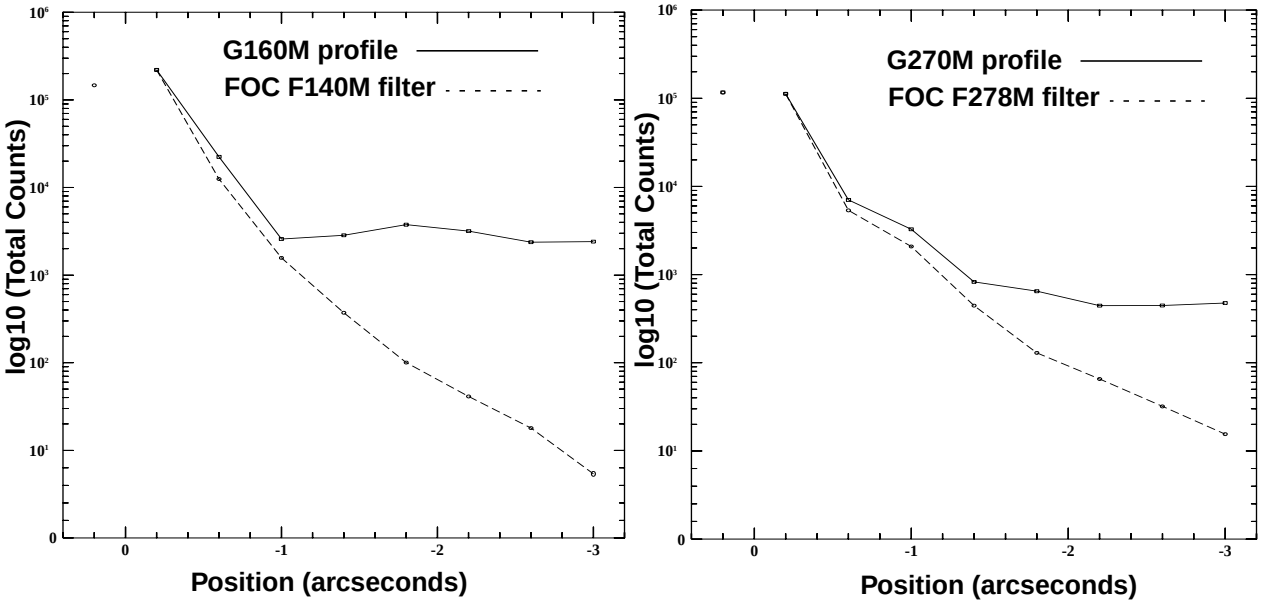

38.2 The GHRS Line Spread Function

The line spread functions (LSFs) for the GHRS gratings describe the instrumental broadening for a delta-function spectral feature. Knowledge of such a blurring function is necessary for quantitative studies of GHRS spectral line profiles. The resolution element (one diode) for GHRS was matched to the width of the SSA. By using substepping strategies, it is possible to get properly sampled spectra, obtaining the minimum of two sample points per resolution element. A delta-function spectra line observed through the SSA can be described by a Gaussian with a FWHM of about 0.925 diodes which is about 3.7 quarter-stepped pixels. (See Gilliland 1992, *PASP*, 104, 367).

Since an SSA spectrum is the best resolution we can obtain with GHRS, it is useful to describe the LSA LSF in terms of the SSA PSF. Consequently, we have measured the LSA-SSA differential LSF for a number of gratings and at a sample of wavelengths. This differential LSF satisfies the relationship: LSF * SSA = LSA; i.e., the differential LSF is the LSF that when convolved with an observed SSA spectrum produces the best match to an identical spectrum obtained through the LSA. By combining the intrinsic LSF for the SSA with the empirical differential LSF we can obtain the intrinsic LSF for the LSA. Since the SSA and differential LSF are Gaussians, we obtain an LSA LSF that is also a Gaussian with a FWHM that is slightly greater than that of the SSA.

The pre-COSTAR LSF of the GHRS was characterized by a Gaussian core nearly twice as broad as that provided by the instrumental resolution limit, provided by the SSA, with extended non-Gaussian wings. The post-COSTAR

LSF for the LSA is only 19–51% broader in a Gaussian core than spectra from the SSA and the extended wings are absent. The LSF results are presented in *GHRS ISR* 063. The differential degradation of the LSF due to the LSA with respect to the LSF of the SSA was derived. A spectral line of a point source with an infinitesimal line width (delta function) measured with the SSA has an LSF with a full width at half maximum (FWHM) of 0.925 diodes. This is independent of wavelength and grating. Measurements of the differential LSF of the LSA were performed for the five wavelength/grating combinations listed in Table 38.1. Column 3 of this table gives the measured FWHM of the differential LSF. Adding this value in quadrature to the FWHM of the SSA LSF (=0.925 diodes) leads to the FWHM of the LSA LSF, given in column 4 of the table. Plots showing the differential LSFs are in *GHRS ISR* 063. No reliable measurements of the LSF for the G140L grating are available. It is very likely that the G140L LSF is similar to those of other gratings.

Table 38.1: GHRS Post-COSTAR Differential LSF

Grating	Wavelength (Å)	Differential LSF of the LSA (diodes)	Relative FWHM (LSA/SSA)
G160M	1360	0.60	1.10
G160M	1900	0.72	1.18
G200M	1900	0.60	1.10
ECH-B	1900	0.82	1.24
ECH-B	2680	0.60	1.10

Deconvolution of GHRS spectra was investigated after the spherical aberration was found in the primary mirror. With COSTAR, the need for deconvolution has become less pressing, however, for the best spectral resolution, it is possible to deconvolve LSA spectra to the level of SSA spectra. See, *The Restoration of HST Images and Spectra*, (proceedings of the HST Calibration Workshop at STScI), STScI, 1990. The STSDAS task, **lucy**, can be used to deconvolve GHRS spectra.